Perpendicular magnetic anisotropy, domains, and misfit strain in epitaxial $Ni/Cu_{1-x}Ni_x/Cu/Si$ (001) thin films

Gabriel Bochi, C. A. Ballentine, H. E. Inglefield, C. V. Thompson, and R. C. O'Handley
Department of Materials Science and Engineering, Massachusetts Institute of Technology, Cambridge, Massachusetts 02139

Hans J. Hug, B. Stiefel, A. Moser, and H.-J. Güntherodt
Institut für Physik, Universität Basel, Klingelbergstrasse 82, CH-4056 Basel, Switzerland
(Received 10 March 1995)

We have investigated the magnetic anisotropy in epitaxial $Ni/Cu_{1-x}Ni_x/Cu/Si$ (001) thin films ($0<x<50\%$) as a function of Ni thickness h and alloy substrate composition. Also the average in-plane biaxial strain $e_0(h)$ in Ni/Cu (001) ($x=0$) was measured *ex situ* versus Ni thickness using optical interferometry. We observed that the preferred direction of magnetization is perpendicular to the films over an exceptionally broad Ni thickness range for films kept under UHV: $10\ \text{Å}<h<60\ \text{Å}$ in Ni/Cu (001); $20\ \text{Å}<h<40\ \text{Å}$ in $Ni/Cu_{60}Ni_{40}/Cu$ (001). We have also studied the perpendicular magnetic anisotropy by magnetic force microscopy and observed a complex domain pattern characterized by two length scales and very strong contrast. We have analyzed our results using a phenomenological model that includes the bulk magnetoelastic anisotropy energy ($B^b e_0$) and both the surface magnetocrystalline (K^s/h) and the surface magnetoelastic ($B^s e_0/h$) anisotropy energies. Our analysis yields the magnetic surface energies K^s and B^s of the vacuum/Ni (001) and Ni/Cu (001) interfaces. The origin of the strong perpendicular magnetic anisotropy lies in the surface energy K^s corresponding to the Ni/Cu (001) interface and the bulk magnetoelastic anisotropy energy. The surface magnetoelastic anisotropy energy $B^s e_0$ favors an in-plane magnetization. The effective magnetoelastic coupling coefficient depends strongly on h for $h \leq 150$ Å and changes sign near $h \approx 28$ Å. The two observed in-plane to out-of-plane magnetization easy-axis transition thicknesses are predicted by our pheomenological model. The lower magnetization easy-axis transition is not due to the onset of misfit dislocations at the Ni/Cu interface.

I. INTRODUCTION

The issue of perpendicular magnetic anisotropy (PMA) in ultrathin films is a very challenging concept since the magnetostatic anisotropy energy always favors an in-plane magnetization easy axis. Considerable experimental effort has been focused on PMA since the pioneering work of Gradmann[1] and the theoretical predictions of Gay and Richter[2] and more recently Freeman and Wu.[3] The most important heteroepitaxial systems that have been investigated and that have exhibited a strong PMA are bcc Fe/Ag (001),[4–8] fcc Fe/Cu (001),[9–14] Co/Pd superlattices,[15,16] Co/Au (111) thin films and superlattices,[17–19] Ni/Cu (001),[20–22] Ni/Cu (111),[20,22] and Cu/Ni/Cu (001) sandwiches.[23–25] In other epitaxial systems, such as fcc Co/Cu (001) thin films,[26,27] fcc Co/Cu (111) superlattices,[17] and fcc Co/Ag (111) superlattices,[19] no experimental evidence of perpendicular magnetization has been found.

In most of the epitaxial structures exhibiting perpendicular magnetization, PMA was found to dominate only over a small film thickness range. For example, in bcc Fe/Ag (001) thin films, the region of perpendicular magnetization extends from $h_{Fe} \approx 5$ Å to $h_{Fe} \approx 9$ Å; in fcc Fe/Cu (001) PMA dominates the magnetic anisotropy for $4\ \text{Å}<h_{Fe}<11$ Å; in Co/Pd superlattices the extent of the perpendicular region depends strongly on the crsytallographic orientation and is largest for the (111) multilayers ($0<h_{Co}<23$ Å).[15] In the present paper, we will show that the Ni/Cu (001) epitaxial system exhibits the largest thickness range of perpendicular magnetization of any epitaxial thin-film system reported so far. Although remarkable, this epitaxial system has received inadequate attention in the literature; this may be due to the relatively small magnetic moment of Ni compared to that of Fe ($\mu_{Ni} \approx 1/3\,\mu_{Fe}$), to the relatively small Curie temperature of Ni ($T_c = 354\,°C$), and/or to the potential growth problems of Ni thin films on Cu substrates, namely segregation of Cu atoms at the surface of Ni [as in Fe/Cu (Ref. 14)]. However, the Ni/Cu (001) epitaxial system is very appealing for the study of magnetic anisotropy in thin films for three reasons. First, Ni has a relatively small magnetostatic energy density [$K^{MS}(Ni) \approx 1/10 K^{Ms}(Fe)$], which constitutes the main resistance to perpendicular magnetization. Second, Ni has a large positive bulk magnetoelastic coupling coefficient so the tendency toward PMA in Ni/Cu is enhanced ($K^{ME} \approx 10^6$ erg/cm^3 for a misfit tensile strain $e_0 = 2\%$). Finally, the Ni/Cu (001) system has a relatively small lattice mismatch (2.6%) which results in a reasonable thickness range for coherent growth ($0<h<18$ Å) and favors good epitaxy.

The published analyses on the behavior of the magnetic anisotropy in epitaxial Ni thin-film systems has often been limited to qualitative arguments. There has been some indirect evidence to suggest that the onset of perpendicular magnetization in Ni/Cu (001) at $h \approx 10$ Å is

0163-1829/95/52(10)/7311(11)/$06.00

associated with the appearance of misfit dislocations.[20] The thickness range over which PMA dominates often has been attributed to the strength of the uniaxial magnetic surface anisotropy (due to the broken symmetry at the film's interfaces)[21–23] or to the magnitude of the misfit strain coupling through the magnetostriction.[21,24,28] The upper thickness limit to the perpendicular region is generally accepted to be due to the strength of the magnetostatic energy. Very few research groups have achieved a quantitative understanding of the behavior of the effective magnetic anisotropy in ultrathin magnetic films through a thorough characterization of their heteroepitaxial structures to include measurements of the saturation magnetization and of the thickness dependence of the strain in the films.[15,17] We have recently measured the thickness dependence of the effective magnetic anisotropy energy in epitaxial Cu/Ni/Cu (001) sandwiches.[25] These measurements indicated that the magnetization is perpendicular to the sandwiches over the thickness range 20 Å $< h_{\mathrm{Ni}} <$ 135 Å. We have analyzed our quantitative data using our own measurements of the thickness dependence of the average in-plane biaxial misfit strain $e_0(h)$ and the strain-dependent Néel pair-interaction model developed recently.[29,30] This analysis yielded both the surface magnetocrystalline (K^s) and the surface magnetoelastic ($B^s e_0$) anisotropy energies corresponding to the Ni/Cu (001) interface. We concluded that the origin of the strong PMA in Cu/Ni/Cu (001) can be found in the surface magnetocrystalline anisotropy energy and the bulk magnetoelastic anisotropy energy ($B_1 e_0$). The surface magnetoelastic anisotropy is responsible for keeping the magnetization in-plane for $h_{\mathrm{Ni}} < 20$ Å.

In this paper, we present our results on the behavior of the magnetic anisotropy in Ni(h)/Cu/Si (001) and Ni(h)/$Cu_{60}Ni_{40}$/Cu/Si (001) thin films characterized *in situ* using the magneto-optic Kerr effect (MOKE), and 100 Å Ni/$Cu_{1-x}Ni_x$/Cu/Si (001) thin films characterized *ex situ* using a vibrating sample magnetometer (VSM). The reason for studying the Ni films on Cu-Ni alloy substrates was to probe further the effects of altering the misfit strain, of changing the critical thickness for the misfit dislocation formation, and of modulating the Ni-substrate magnetic interfacial anisotropy. Magnetic force microscopy was used to probe the magnetic domain structure in these films. We have also imaged misfit dislocations (MD's) at the Ni-Cu interface and measured the Ni thickness dependence of the average in-plane biaxial misfit strain in Ni/Cu/Si (001) thin films. The combination of the magnetic and structural characterizations confirm the roles played by the bulk magnetoelastic anisotropy and the surface magnetocrystalline anisotropy in governing the strong PMA in Ni/Cu (001). We also discuss the role played by the onset of interfacial MD's in the magnetization easy-axes transitions.

II. GROWTH AND STRAIN RELAXATION IN Ni/$Cu_{1-x}Ni_x$/Cu/Si (001)

The Ni/$Cu_{1-x}Ni_x$/Cu (001) thin films were evaporated at room temperature on Si (001) wafers using a molecular-beam-epitaxy (MBE) deposition system. The Ni film thickness ranged between 10 and 150 Å whereas the $Cu_{1-x}Ni_x$ layers were 1000 Å thick. The 1000 Å Cu buffer layer was needed to make possible the epitaxial growth of the $Cu_{1-x}Ni_x$ layers with a (001) orientation on Si(001). More details on the sample preparation and evaporation conditions can be found elsewhere.[21,31] The structure and chemistry of the films were characterized *in situ* using reflection high-energy electron diffraction (RHEED) and Auger electron spectroscopy and *ex situ* using plan-view and cross-sectional transmission electron microscopy (TEM), x-ray diffraction, and optical interferometry to measure the thickness dependence of the strain in the Ni films. Following the deposition, the magnetic anisotropy of the films was characterized *in situ* using MOKE and *ex situ* using VSM.

In agreement with the observations of Naik *et al.*,[23] our RHEED patterns and x-ray pole figures indicated that the Ni and Cu films grow epitaxially with a (001) orientation and with their [100] axis parallel to the [110] axis of the Si wafer. This 45° rotation of the films about their normal decreases the huge lattice mismatch ($\approx 50\%$) between Cu and Si to approximately 6%, thus making the epitaxial growth of Cu(001) on Si(001) possible. The cross-sectional TEM revealed a Ni surface roughness of the order of ± 20 Å with an autocorrelation length of 400 Å in the film plane. The micrographs showed no sign of interdiffusion at the Ni-Cu interface in agreement with the results of Mankey, Kief, and Willis[32] and Chen *et al.*[33]

Using plane-view TEM, we have resolved both 60° and 90° MD's at the Ni/Cu (001) interface and we measured the MD density as a function of Ni film thickness.[31,34] We found that the MD's roughly form an orthogonal grid at the Ni-Cu interface, run along the ⟨110⟩ directions and are either 60° type or 90° type. MD's were present in Ni/Cu (001) thin films having Ni thicknesses 25 Å and greater but not in the films having 15 Å of Ni. This indicates that the critical thickness h_c for the onset of MD's is between 15 and 25 Å. This result is in agreement with an earlier TEM work,[35] where it was shown that $h_c \approx 15 \pm 3$ Å, and with the theoretical prediction, $h_c = 18$ Å, of the Matthews-Blakeslee thermodynamic model.[36] Although this model has some limitations, it yields some important and useful results on the strain relaxation in thin films which have not received adequate attention in the literature and which are relevant to the present work. We therefore review them briefly with a specific aim to determine the predictions of this simple model with regard to misfit strain accommodation for epitaxial Ni films grown on various Cu-Ni alloy substrates.

In the early stages of epitaxy, i.e., when $h_{\mathrm{Ni}} < h_c$, the Ni film is pseudomorphic with the Cu substrate and it experiences an anisotropic strain: the film is under an in-plane biaxial tensile misfit strain given by $e_0 = \eta$, where η is the Ni-Cu lattice mismatch; it also experiences a Poisson compression along its normal given by $e_0' = -\eta$ (Refs. 29 and 30) in addition to any surface relaxation.[37] The critical thickness for the onset of MD's is given by[36]

$$h_c = \frac{b}{8\pi\eta\cos\lambda}\left[\frac{1-\nu\cos^2\beta}{1+\nu}\right]\ln\left[\frac{4h_c}{b}\right], \qquad (1)$$

where b is the magnitude of Burgers vector. This vector **b** makes an angle of λ with the direction that is both perpendicular to the dislocation direction ξ, and that lies in the plane of the interface. Only the component $b\cos\lambda$ acts to relieve lattice misfit strain. β is the angle given by $\cos\beta=\xi\cdot\mathbf{b}/b$. In fcc crystals, such as Ni, the majority of the MD's are characterized by $\beta=\lambda=60°$ and the Burgers vectors are of the $\frac{1}{2}\langle 110\rangle$ type, yielding $b=(1/\sqrt{2})a_0$ (film). Above the critical thickness ($h>h_c$), the dislocated film is more stable than the coherently strained film: the energy gained from misfit strain relief is larger than the energy cost associated with the introduction of interfacial MD's. The dislocation linear density increases as the film thickness h gets larger. Simultaneously, the residual average in-plane biaxial misfit strain decreases with h as follows:

$$e_0(h)=\eta\frac{h_c}{h}\frac{\ln(4h/b)}{\ln(4h_c/b)}\ , \quad h>h_c\ . \tag{2}$$

This strain can be approximated by

$$e_0(h)=\eta\frac{h_c}{h}\ , \quad h>h_c\ , \tag{3}$$

which has been proposed by Chappert and Bruno[38] and has frequently been referred to in the thin film magnetism community. Thus Eqs. (1) to (3) predict a constant misfit strain $e_0=\eta$ for epitaxial films up to $h=h_c$ and a decreasing strain $e_0(h)\approx\eta(h_c/h)$ for $h>h_c$.

A very important corollary follows from Eqs. (1) and (2). Consider Ni thin films grown epitaxially on two different substrate such as Cu (001) and $Cu_{1-x}Ni_x$ (001). Then, according to Eqs. (1) and (2), for $h<h_c$, the average in-plane biaxial tensile misfit strain in the Ni/Cu (001) and the Ni/$Cu_{1-x}Ni_x$ (001) films is η_1 and η_2, respectively, with $\eta_1=2.6\%>\eta_2$. However, for $h>h_c$\{Ni/$Cu_{1-x}Ni_x$ (001)\} the strain in the Ni film is the same in Ni/Cu (001) and in Ni/$Cu_{1-x}Ni_x$ (001). This result is illustrated graphically in Fig. 1 for Ni/Cu (001) and Ni/$Cu_{60}Ni_{40}$ (001) for which the lattice mismatch is 2.6 and 1.6%, respectively, and the critical thickness is 18 and 35 Å, respectively. A phase digram showing the critical thickness h_c and the lattice mismatch η corresponding to Ni thin films grown epitaxially on $Cu_{1-x}Ni_x$(001) substrates for $0<x<50\%$ is shown in Fig. 2. It was obtained using Eq. (1) and assuming that Ni and Cu form a solid solution in the bulk at room temperature.

Quantitative measurements of strain relaxation in the Ni/Cu epitaxial system were carried out by Gradmann[1] for films grown with a (111) orientation. Matthews and Crawford[35] studied the accommodation of misfit strain in epitaxial Ni/Cu (001) thin films evaporated on NaCl (001) substrates. Bruno and Renard[39] showed that the elastic-strain data of Matthews and Crawford can be reasonably fit by the $1/h$ functional form of Eq. (3) for Ni thicknesses up to 100 Å. We also measured recently the misfit strain accommodation in Ni/2000 Å Cu/Si (001) thin films using a WYKO 6000 PC optical interferometer.[34] This instruments uses optical reflection from a Si wafer compared with the reflection from a flat reference

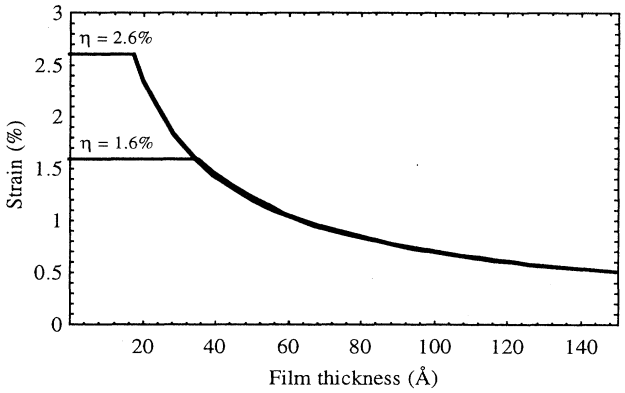

FIG. 1. Average in-plane biaxial misfit strain as a function of Ni film thickness for Ni/Cu (001) ($\eta=2.6\%, h_c=18$ Å) and for Ni/$Cu_{60}Ni_{40}$ (001) ($\eta=1.6\%, h_c=35$ Å), according to Eqs. (1) and (2).

to determine the curvature of the Si wafer. By measuring the curvature of the wafer before and after deposition of the Cu layer, one can determine the curvature caused by the 2000 Å Cu layer. The curvature of the Ni/2000 Å Cu/Si (001) thin films was similarly obtained for different Ni film thicknesses. By subtracting the "background" curvature due to the Cu layer, one obtains the effective change in curvature $\Delta\kappa$ of the Si wafer due to the Ni film. A modified version of Stoney's equation can then be used to find the residual elastic strain in the Ni films as a function of Ni thickness. The results are shown in Fig. 3. The solid line in this figure is the best fit of the data points using a power law. The equation of the line is given by

$$e_0\approx\frac{18}{h^{0.70}}\ , \quad h>h_c\ , \tag{4}$$

where e_0 is expressed in percent and where h is in Angstroms. The functional form of Eq. (4) is relatively close to that of the Chappert-Bruno model of Eq. (3). These data are important input to a full understanding of the behavior of the magnetic anisotropy in Ni/$Cu_{1-x}Ni_x$ (001) epitaxial thin films.

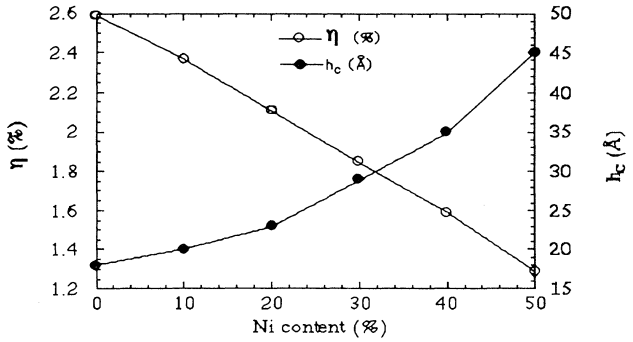

FIG. 2. Lattice mismatch and critical thickness in Ni/$Cu_{1-x}Ni_x$ (001) as a function of Ni content (x) in the substrate, according to Eq. (1).

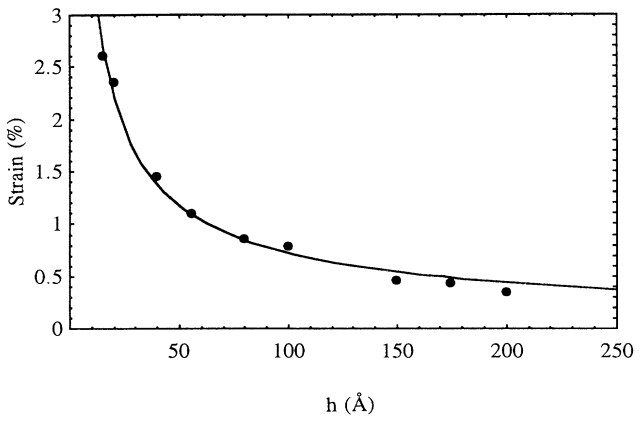

FIG. 3. Thickness dependence of the strain in Ni/2000 Å Cu/Si (001) thin films measured by optical interferometry. The solid line represents the best fit to the data points using a power-law functional form which is given by Eq. (4).

III. MAGNETIC ANISOTROPY

A. Ni/Cu (001) thin films

1. Experimental results

The first structure that we examined was epitaxial Ni/Cu/Si (001). The films were characterized both *in situ* and *ex situ*. Representative *in situ* MOKE loops obtained with the magnetic field applied in the film plane and perpendicular to it are shown in Figs. 4(a)–4(c). The *M-H* loops corresponding to the 150, 100, and 75 Å thick films are very similar and indicate that the magnetization easy axis lies in the film plane. In fact, the remanence of the loops taken with the magnetic field applied in-plane is relatively large whereas the loops taken with the field normal to the films exhibit a linear behavior and an insignificant remanence which are characteristic of hard-axis *M-H* loops. This result is not surprising since the magnetostatic energy, which tries to keep the magnetization in-plane, always dominates at sufficiently large film thicknesses. The magnetic anisotropy changes dramatically when the Ni film thickness is decreased below 60 Å,

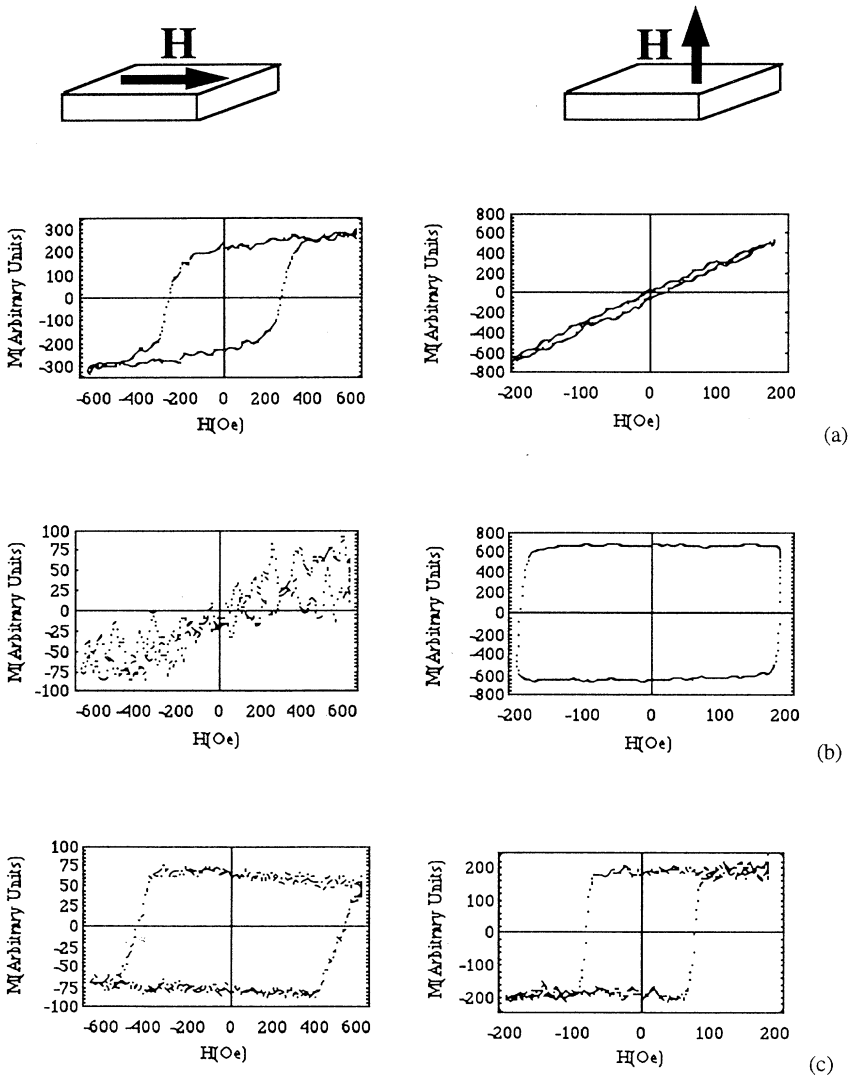

FIG. 4. (a) Longitudinal and polar MOKE loops of a 100 Å Ni/Cu/Si (001) film. (b) Longitudinal and polar MOKE loops of a 50 Å Ni/Cu/Si (001) film. (c) Longitudinal and polar MOKE loops of a 15 Å Ni/Cu/Si (001) film.

as indicated by Figs. 4(b) and 4(c). The polar M-H loops corresponding to the 50, 35, and 25 Å thick films are square and have a 100% remanence, indicating that the magnetization easy axis is normal to the films. The corresponding longitudinal M-H loops are linear and have essentially zero remanence.

We have observed another significant change in the magnetic anisotropy at a Ni thickness between 10 and 15 Å. As indicated by Fig. 4(c), both the polar and the longitudinal M-H loops appear to have 100% remanence up to the fields indicated when the Ni film thickness is $h=15$ Å. Such a situation can be explained if the 15 Å Ni film is either discontinuous or continuous but rough, with islands or regions magnetized in-plane and others magnetized perpendicular to the film. The roughness of the Ni/Cu (001) films has been confirmed by RHEED and cross-sectional TEM to be of order ± 20 Å, as explained above. This mixed behavior of the magnetic anisotropy at $h=15$ Å, which we reported earlier,[21] has been confirmed by Huang *et al.*[22] who have deposited their films at room temperature on Cu (001) single-crystal substrates and characterized them at $T=160$ K by MOKE. Huang *et al.* further demonstrated that the magnetization easy axis falls completely in-plane below $h=13$ Å. This transition of the magnetization easy axis from in-plane to perpendicular, observed in ultrathin Ni, supports the earlier results of Ballentine.[20] In fact, by depositing his Ni/Cu (001) films at room temperature and characterizing them at $T=100$ K with MOKE, Ballentine showed that the magnetization lies fully in-plane for $h=5.5$ Å and exhibits a strong out-of-plane component for $h=8.3$ Å. We tried to study this in-plane to out-of-plane magnetization easy-axis transition with our MOKE setup by depositing Ni films thinner than 15 Å. However, MOKE measurements at these thicknesses and at room temperature are very difficult since the saturation magnetization is very small, making the Kerr rotation very weak. Tjeng *et al.*[40] and Huang *et al.*[22] showed that the Curie temperature of 9 Å thick Ni films deposited on Cu (001) substrates is $T_c \approx 300$ K.

Following the MOKE measurements, the Ni/Cu/Si (001) films were brought up to air and characterized by VSM. For films deposited by MBE and then exposed to air, the upper limit to the region of perpendicular magnetization shifts from 60 to approximately 125 Å. This significant difference between films characterized under vacuum and films characterized by VSM is due to the exposure of the films to air. In fact, when a 75 or a 100 Å thicken Ni film is exposed to air and then returned to the MBE chamber, the MOKE loops indicate that the magnetization easy axis remains perpendicular to the film plane. The cause of the shift in the upper thickness limit of the perpendicular magnetization region upon exposure to air is beyond the scope of the present paper. However, it can be speculated that it is due to a combination of any of the following three possibilities: a loss of the Ni moment due to a significant oxidation of the Ni film, leading to a decrease of the magnetostatic energy of the film; a tensile stress imposed on the Ni film by the growing oxide leading to an increase of the positive bulk magnetoelastic anisotropy energy $2B_1e_0$ of the Ni film; and/or a significant increase in the magnetic surface anisotropy energy density K^s of the film due to the coverage of the Ni free surface by the oxide. Cross-sectional TEM studies have shown that the oxide layer growing on the Ni free surface is thinner than 10 Å.[41,42] This would certainly not reduce the Ni moment enough to make a 100 Å oxidized film behave like an unoxidized 50 Å thick film kept under vacuum. However, the other two mechanisms remain possible and could act simultaneously.

In order to better understand the strong PMA implied by the above *in situ* MOKE loops [Figs. 4(a)–4(c)] and by our *ex situ* VSM measurements on epitaxial Cu/Ni/Cu (001) sandwiches,[25] we have investigated the magnetic domain structure of our Ni/Cu (001) thin films using a magnetic fore microscope (MFM). The first and most important question that needs to be addressed is whether or not magnetic domains occur at all in our epitaxial thin films since they have been predicted to be forbidden[43] or to occur only under very special conditions.[44] Scanning electron microscopy with spin-polarization analysis (SEMPA) experiments have shown that micron size domains do exist in ultrathin Co/Au (001) films[18] but that ultrathin Co/Cu (001) films grow in a nearly single-domain configuration.[45] Since the present MFM measurements are performed *ex situ,* we have imaged Ni/Cu/Si (001) films which were capped by a 20 Å thicken Cu layer in order to protect the Ni films. The energy balance in Cu/Ni/Cu (001) sandwiches is similar to that of the Ni/Cu (001) films that form the main subject of this work. The PMA is even stronger when the Ni/Cu (001) films are capped with Cu and dominates the total magnetic anisotropy up to Ni thicknesses $h \approx 135$ Å.[25]

In magnetic force microscopy experiments, a tiny ferromagnetic tip, integrated into a microfabricated cantilever, is scanned parallel to the surface of a magnetic sample. Note that we use the static, variable reflection measurement mode as described in Refs. 46 and 47. The stray field emanating from the sample, $\mathbf{H}_{\text{Sample}}$, interacts with the magnetized tip, giving a fore

$$F_z = -\mu_0 \int_{V_{\text{Tip}}} \left[\mathbf{M}_{\text{Tip}} \cdot \frac{\partial}{\partial z} \mathbf{H}_{\text{Sample}} \right] dV \ , \tag{5}$$

where the integration is performed over the tip volume, V_{Tip}, with the magnetization $\mathbf{M}_{\text{Tip}}$. In order to achieve a resolution of a few tens of nanometers and to have direct access to the local magnetization of the sample, we have electron-beam deposited an approximately long carbon contamination needle on the top of a commercial microfabricated silicon nitride atomic force microscopy cantilever tip. The nonmagnetic needle is coated from one side by a 25 nm thick $Co_{80}Ni_{20}$ magnetic thin film by electron beam deposition. The radius of curvature of the tip is less than 40 nm.[48] Such a magnetic layer is expected to be in a monodomain state with the magnetization parallel to the tip axis and thus perpendicular to the plane of the film.[48,49] At a tip-to-sample distance in the range of 10 to 20 nm, the force acting on the tip [Eq. (5)] is mainly due to the magnetic surface charge, $\rho_{m,\text{Tip}}$, at the tip end close to the sample. Equation (5) then reduces to

$$F_z \approx \int_{A_{\text{Tip,Front}}} (\rho_{m,\text{Tip}} \cdot H_{z,\text{Sample}}) dA \ , \quad (6)$$

where the magnetic charge at the lower tip end is given by $\rho_{m,\text{Tip}} = M_{z,\text{Tip}} \cdot A_{\text{Tip,Front}}$. The force map of the scanned surface, $F_z(x,y)$, is expected to show attractive or repulsive areas if the local direction of the magnetization of the sample is parallel or antiparallel, respectively, to the magnetization of the tip. No z-directed force is expected if the sample is locally magnetized in-plane.

The image in Fig. 5(a) is an MFM measurement on a demagnetized 100 Å Ni/Cu/Si (001) film capped by a 20 Å Cu layer. Clearly a complex pattern of perpendicular domains magnetized into and out of the film plane is observed. No in-plane magnetization regions are observed; the measured force is either into or out of the film. The domain pattern shows two length scales: a coarse, serpentine pattern having a width of order 2 μm and a finer bubblelike pattern with submicron dimensions. These interesting features are not yet understood. The remanent domain state after saturation is also of interest. The sophisticated construction of the force microscope used here, which will be described elsewhere, allows the sample to be removed, magnetized, and replaced in the microscope to reobserve in the remanent state the same sample area previously imaged. The image in Fig. 5(b) is the image after exposing the sample to a field of 4000 Oe pointing into the plane of the 100 Å Ni sandwich. Clearly, the total area of out-of-plane domains is drastically reduced; the remanence is approximately 75% of saturation.

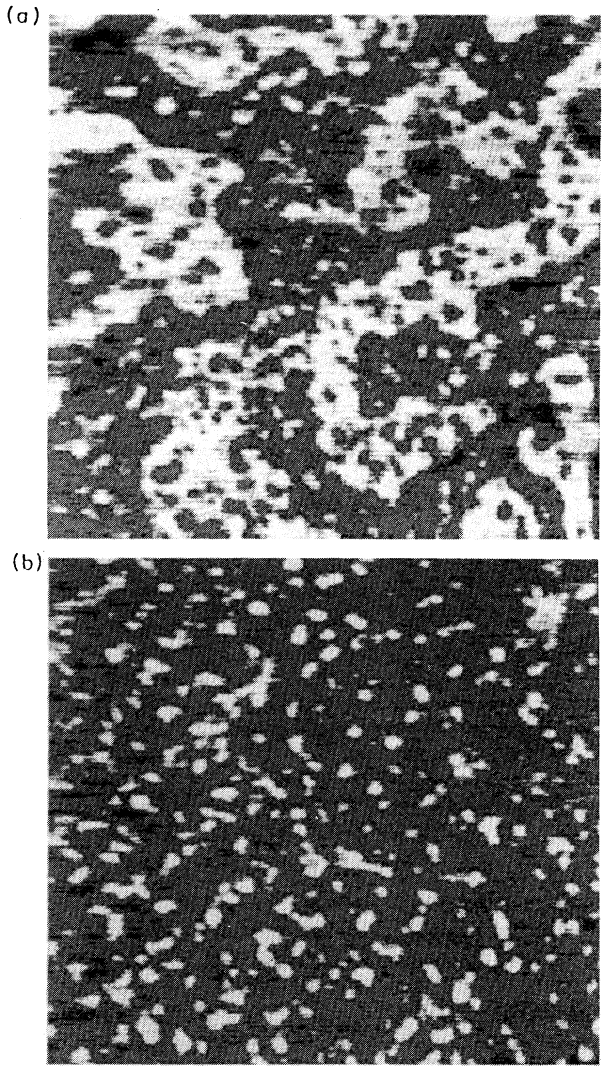

FIG. 5. (a) MFM image of the magnetic domain structure of a 20 Å Cu/100 Å Ni/2000 Å Cu/Si (001) sandwich. The light regions are perpendicular domains magnetized out of the plane of the film whereas the dark regions are perpendicular domains magnetized into the plane of the film. The up and down domains cover comparable surface areas indicating that the sandwich is demagnetized; (b) MFM images of the same sandwich after exposing it to a 4000 Oe magnetic field pointing into the plane of the film. The up domains shrink whereas the down domains grow. The field of view in both images is 10 μm $\times$ 10 μm.

Figure 6 shows also a 10 μm $\times$ 10 μm region of an 85 Å Ni/Cu/Si (001) film capped by a 20 Å Cu layer. Despite the 15% decrease in Ni film thickness here there is no significant decrease in contrast. The domain structure is simpler than the one in Fig. 5(a); only the large scale serpentine pattern is observed. This is probably due to the reduced magnetostatic energy and to the increased effective magnetic anisotropy at the smaller Ni thickness.[25]

To summarize the domain images, our films are multidomain in the perpendicular thickness range. MFM is able to image domains in Cu/Ni/Cu/Si (001) films with Ni thicknesses at least as low as 85 Å. To our knowledge, all previous MFM measurements have been made on much thicker films or bulk samples. A more detailed discussion of the domain images on the films described here as well as others will be presented in forthcoming publications.

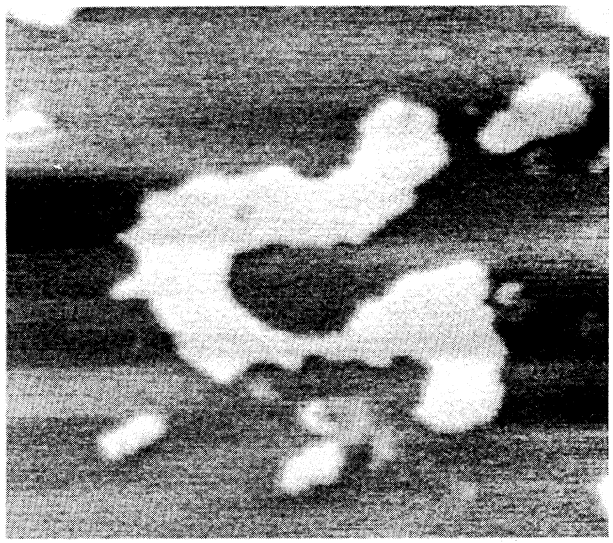

FIG. 6. MFM image of 20 Å Cu/85 Å Ni/2000 Å Cu/Si (001) sandwich. As in Fig. 5, the field of view of 10 μm $\times$ 10μm.

2. *Phenomenological analysis*

In order to extract the value of the magnetic surface anisotropy energies K^s corresponding to the vacuum/Ni/Cu (001) epitaxial system, it is imperative that we review briefly the appropriate phenomenological model. We have recently analyzed the behavior of the effective magnetic anisotropy energy density K^{eff} as a function of Ni film thickness in epitaxial Cu/Ni/Cu (001) sandwiches.[25] We showed that $K^{\text{eff}}(h)$ cannot be described without the inclusion of the *surface magnetoelastic anisotropy* term predicted by the strain-dependent Néel model.[29] The complete phenomenological equation that best describes the magnetic anisotropy in epitaxial Cu/Ni/Cu (001) sandwiches is given by[30]

$$K^{\text{eff}} = -2\pi M_s^2 + 2B_1 e_0(h) + 2\frac{B^s}{h} e_0(h) + 2\frac{K^s}{h} , \quad (7)$$

where B_1 is the bulk magnetoelastic coupling coefficient of Ni ($B_1 = 6.2\times 10^7$ erg/cm^3). B^s and K^s are the strain-dependent and strain-independent magnetic surface anisotropies corresponding to the Ni/Cu (001) interface, respectively. B^s is also called the surface magnetoelastic coupling coefficient. The bulk magnetocrystalline anisotropy of Ni is negligible and has therefore been omitted in Eq. (7). Our analysis of the $K^{\text{eff}}(h)$ data of Cu/Ni/Cu (001) sandwiches using Eq. (7) yielded $K^s \approx +0.85$ erg/cm^2 and $B^s \approx -50$ erg/cm^2 for the Ni/Cu (001) interface. We use Eq. (7) and the data of the previous section to obtain the two magnetic surface anisotropy energies corresponding to the Ni/vacuum (001) interface.

Our *in situ* magnetic field were not large enough to saturate the *M-H* loops and hence inadequate to measure $K^{\text{eff}}(h)$ for our vacuum/Ni/Cu (001) films. However, we can analyze the above data by exploring the fact that $K^{\text{eff}} = 0$ at the transition thicknesses between the perpendicular and in-plane magnetization regions. The two magnetization easy-axis transition thickness are $h_1 = 15$ Å and $h_2 = 60$ Å in vacuum/Ni/Cu (001). Substituting $K^{\text{eff}} = 0$ and the strain of Eq. (3) into Eq. (7) yields

$$2\pi M_s^2 \cdot h^2 = [2B_1 \eta h_c + 2\langle K^s \rangle]h + 2\langle B^s \rangle \eta h_c , \quad h > h_c , \quad (8)$$

for the vacuum/Ni/Cu (001) epitaxial system. Here the surface energies are expressed as averages over the Ni/vacuum and the Ni/Cu interfaces:

$$\langle K^s \rangle = \frac{K^s(\text{Ni/vacuum}) + K^s(\text{Ni/Cu})}{2} \quad (9)$$

and

$$\langle B^s \rangle = \frac{B^s(\text{Ni/vacuum}) + B^s(\text{Ni/Cu})}{2} . \quad (10)$$

Equation (8) applies at both transition thicknesses, h_1 and h_2. With two equations and two unknowns, $\langle K^s \rangle$ and $\langle B^s \rangle$, we determined the two magnetic surface anisotropy energies corresponding to the combination of the Ni/vacuum (001) and Ni/Cu (001) interfaces uniquely: $\langle K^s \rangle \approx +0.32$ erg/cm^2 and $\langle B^s \rangle \approx -17$ erg/cm^2. Using the surface energies determined for the Ni/Cu (001) interface,[25] we deduced: $K^s(\text{Ni/vacuum})\ (001) \approx -0.21$ erg/cm^2 and $B^s(\text{Ni/vacuum})(001) \approx +15$ erg/cm^2. The magnetic surface anisotropy energies corresponding to the Ni/Cu (001) and Ni/vacuum (001) interfaces are summarized in Table I. The negative value for K^s(Ni/vacuum) (001) is consistent with the early predictions of in-plane magnetization for a free standing Ni monolayer.[2] Also K^s and B^s have opposite signs for both the Ni/vacuum (001) and the Ni/Cu (001) interfaces, in agreement with the predictions of the strain-dependent Néel pair-interaction model.[29]

TABLE I. Summary of the surface magnetocrystalline energies and the surface magnetoelastic coupling coefficients obtained in this work.

Anisotropy energy/ interface	K^s (erg/cm^2)	B^s (erg/cm^2)
Ni/vacuum (001)	−0.21	+15
Ni/Cu (001)	+0.85	−50

Using the magnetic surface energies of Table I, we plot in Fig. 7 the magnetic anisotropy energy densities that are responsible for PMA in vacuum/Ni/Cu (001). From this figure, we conclude that the origin of PMA in vacuum/Ni/Cu (001) thin films, as in the Cu/Ni/Cu (001) sandwiches,[25] resides in the positive bulk magnetoelastic anisotropy energy, $2B_1 e_0(h)$, and in the positive average surface magnetocrystalline anisotropy energy of the Ni film. The negative average surface magnetoelastic anisotropy energy is responsible for bringing the magnetization easy-axis in-plane for $h < 15$ Å. The upper magnetization easy-axis transition thickness ($h \approx 60$ Å) in vacuum/Ni/Cu (001) is due to the magnetostatic energy $2\pi M_s^2$. Finally, the average negative surface magnetoelastic coupling coefficient, $\langle B^s \rangle \approx -17$ erg/cm^2, corresponding to the combination of the Ni/vacuum (001) and Ni/Cu (001) interfaces, implies that the effective magnetoelastic coupling coefficient in vacuum/Ni/Cu (001) films, $B^{\text{eff}} = B_1 + \langle B^s \rangle / h$, changes sign at $h \approx 28$ Å. In Cu/Ni/Cu (001) sandwiches, we showed that B^{eff} changes

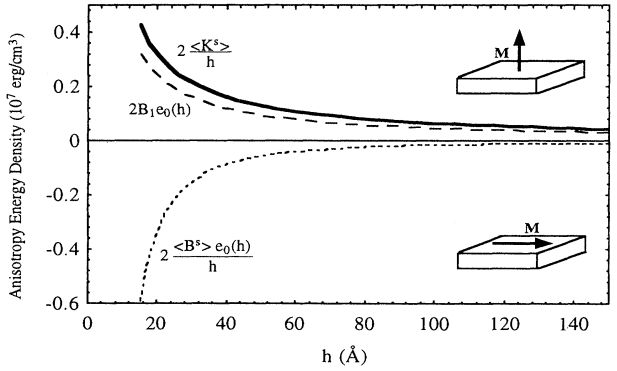

FIG. 7. Dependence of three different magnetic anisotropy energies on Ni film thickness in vacuum/Ni/Cu (001) thin films. We use the magnetic surface anisotropy energies of Table I to compute $\langle K^s \rangle$ and $\langle B^s \rangle$. The figure shows that the bulk magnetoelastic and the average surface magnetocrystalline anisotropies constitute the origin of the PMA in vacuum/Ni/Cu (001).

sign at $h \approx 80$ Å.[25] Using direct *in situ* methods, Song, Ballentine, and O'Handley[50] and Weber, Koch, and Rieder[51] recently measured the effective magnetostriction constants of polycrystalline NiFe alloys and polycrystalline iron. In both cases, the magnetoelastic coupling changed sign from its bulk value at large film thickness to opposite values at small thickness. The sign change occurs at magnetic film thicknesses in the range 30 Å $< h <$ 80 Å.

Although the magnetization easy axis follows equalitively the same behavior in vacuum/Ni/Cu (001) and Cu/Ni/Cu (001), the Ni thickness dependence of K^{eff} in these two epitaxial systems differs significantly. In Fig. 8, we plot $K^{\text{eff}} \cdot h$ versus h for the sandwiches and the films using Eqs. (7) and (8), respectively, and the magnetic surface anisotropy energies of Table I. The figure clearly suggests two major differences between the two epitaxial systems: the extent of the perpendicular region is much larger in Cu/Ni/Cu (001); the PMA energy in Cu/Ni/Cu (001) is about three times larger than in vacuum/Ni/Cu (001). The origin of these remarkable differences resides in the fact that the total surface magnetocrystalline anisotropy energy in Cu/Ni/Cu (001) is significantly larger than in vacuum/Ni/Cu (001). We have demonstrated experimentally that $K^{\text{eff}} \cdot h$ in Cu/Ni/Cu (001) follows the sold curve in Fig. 8.[25] As far as we knonw, $K^{\text{eff}} \cdot h$ versus h has never been measured quantitatively for vacuum/Ni/Cu(001) thin films.

B. $Ni/Cu_{60}Ni_{40}/Cu$ (001) thin films

It had been suggested that the magnetization easy-axis transition occurring in Ni/Cu (001) at $h \approx 10$–15 Å may be due to the onset of MD's.[20] In order to test this idea, we have studied the magnetic anisotropy in $Ni/Cu_{60}Ni_{40}/Cu/Si$ (001) thin films as a function of Ni thickness. The mismatch between the equilibrium lattice parameters of Ni and $Cu_{60}Ni_{40}$ is approximately 1.6% and the corresponding thermodynamic critical thickness for the onset of MD's is approximately 35 Å (Fig. 2). By

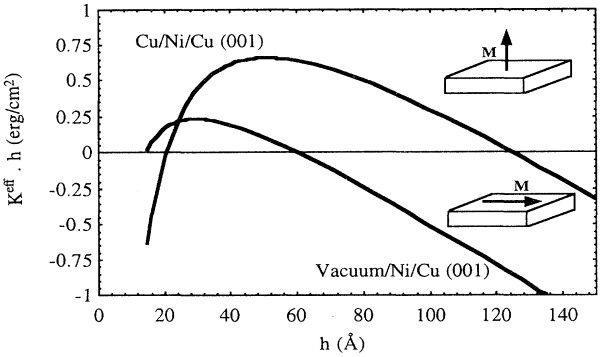

FIG. 8. Dependence of $K^{\text{eff}} \cdot h$ on Ni film thickness, h, in Cu/Ni/Cu (001) sandwiches and vacuum/Ni/Cu (001) thin films according to Eqs. (7) and (8), respectively. The appropriate magnetic surface anisotropy energies can be found in Table I. This figure shows that PMA is larger and dominates over a larger Ni thickness range in the Cu/Ni/Cu (001) sandwiches.

measuring the magnetic anisotropy of Ni thin films deposited on $Cu_{60}Ni_{40}$ substrates for film thicknesses below and above 35 Å, we can determine whether or not the onset of MD's is responsible for the lower magnetization easy-axis transition. The choice of the ally composition was made with two ideas in mind: the Ni content in the substrate must be large to make the critical thickness h_c large (Fig. 2); at the same time, the Ni content in the substrate must be small enough so that the substrate can remain nonmagnetic. The bulk Cu-Ni equilibrium phase diagram indicates that, at room temperature, Ni and Cu form a solid solution which is nonmagnetic provided the Ni content in the alloy is less than 65 at. %. We chose the composition 60% Cu-40% Ni.

The Ni film thickness for these experiments ranged between 15 and 100 Å. Before characterized in the $Ni/Cu_{60}Ni_{40}/Cu/Si$ films, we characterized a $Cu_{60}Ni_{40}/Cu/Si$ film using MOKE. No hysteresis loops were detected indicating that the alloy substrates were nonmagnetic, as expected. Some of the M-H loops of the $Ni/Cu_{60}Ni_{40}/Cu/Si$ (001) thin films, obtained using MOKE while the films were kept under UHV, are shown in Figs. 9(a)–(9(c). The M-H loops indicate that the 100, 75, and 50 Å Ni films have an in-plane magnetization easy axis. The magnetic anisotropy changes significantly around 40 Å. In fact, as can be seen in Figs. 9(b) and 9(c), the magnetization easy axis is normal to the film plane for the 35 and 25 Å films since the remanence of the polar loops is close to 100%. For the 15 Å film, a weak hysteretic behavior is observed both for the magnetic field applied in-plane and perpendicular to the film, indicating that the 15 Å film is ferromagnetic at room temperature and of mixed anisotropy character. The relatively small remanence in the polar loop at 15 Å indicates that the magnetization easy axis may be falling back in-plane at this thickness. However, the weakness of the Kerr signal makes it difficult to draw a stronger conclusion.

Nonetheless, we can draw two major conclusions from Figs. 9(a) to 9(c). First, we have shown that the region of perpendicular magnetization extends from approximately 20 to 40 Å in $Ni/Cu_{60}Ni_{40}/Cu$ (001); this is narrower than the perpendicular region in Ni/Cu (001) films which extends from 15 to 60 Å. Second, the onset of MD's, which is calculated to occur at $h_c \approx 35$ Å, does not appear to be responsible for the lower magnetization easy-axis transition, which occurs near 20 Å. The results of the previous section indicate that the transition is rather due to the change in sign of the effective magnetoelastic coupling coefficient of the films. Two transition thicknesses for the magnetization easy axis have also been observed in bcc Fe/Ag (001) (Ref. 6) and fcc Fe/Cu (001).[10,11] In these two epitaxial systems, the lower transition thickness is $h = 4$–5 Å. However, according to Eq. (1), the critical thickness for the onset of MD's is $h_c = 26$ Å for bcc Fe/Ag (001) ($\eta = 0.8\%$) and $h_c = 38$ Å for fcc Fe/Cu (001) ($\eta = 1.5\%$), both thicknesses being much larger than 5 Å. This observation supports our conclusion that the onset of MD's is not responsible for the in-plane to out-of-plane magnetization easy-axis reversal.

Two factors can explain why the reign of perpendicular magnetization is narrower for the $Ni/Cu_{60}Ni_{40}$ (001) thin films than for the Ni/Cu (001) films. First, the in-plane biaxial tensile misfit strain in the Ni films is smaller in $Ni/Cu_{60}Ni_{40}$ (001) than in Ni/Cu (001). This is due to the fact that Ni has a much smaller misfit with the $Cu_{60}Ni_{40}$ alloy than with a Cu substrate, as illustrated in Figs. 1 and 2. As a result, the bulk magnetoelastic anisotropy energy, which gives rise to an important contribution to the PMA in Ni/Cu (001), is smaller in $Ni/Cu_{60}Ni_{40}$ (001) than in Ni/Cu (001), at least up to approximately 35 Å Ni (Fig. 1). Second, as we showed in the previous section, the surface magnetocrystalline anisotropy energy of the Ni-Cu (001) interface is strong, positive and therefore contributes significantly to PMA in Ni/Cu (001). The $Ni\text{-}Cu_{60}Ni_{40}$ interface is chemically and structurally closer to a Ni-Ni interface (created depositing a Ni thin film on a Ni single-crystal substrate) than the Ni-Cu interface is. To a first approximation, on therefore expects the $Ni\text{-}Cu_{60}Ni_{40}$ (001) interface to have a magnetic surface anisotropy energy density which is closer to zero, i.e., less positive than that of the one of the Ni-Cu (001) interface. In other words, its contribution to the PMA is weaker than that of the Ni-Cu (001) interface, leading to a narrower thickness range for perpendicular magnetization in $Ni/Cu_{60}Ni_{40}/Cu$ (001) compared to Ni/Cu (001).

C. 100 Å $Ni/Cu_{1-x}Ni_x/Cu$ (001) thin films

In order to qualitatively test the effect of the surface magnetocrystalline anisotropy energy of the Ni-Cu (001) interface on the PMA in Ni/Cu (001) thin films, we deposited a series of $Ni/Cu_{1-x}Ni_x/Cu/Si$ (001) films and have characterized them *ex situ* by VSM. Contrary to the samples of section B, the Ni film thickness was fixed here to 100 Å and the alloy composition was varied, never exceeding 50% Ni. The experimental results are shown in Fig. 10, which is a plot of the perpendicular remanence normalized to the saturation magnetization as a function of the Ni content in the substrate expressed in atomic percent. As explained in Sec. III A, a 100 Å Ni thin film deposited under UHV on a pure Cu substrate ($x=0$) and then exposed to air has a perpendicular magnetization easy axis. This is confirmed in Fig. 10.

As the Ni content in the substrate is increased, the per-

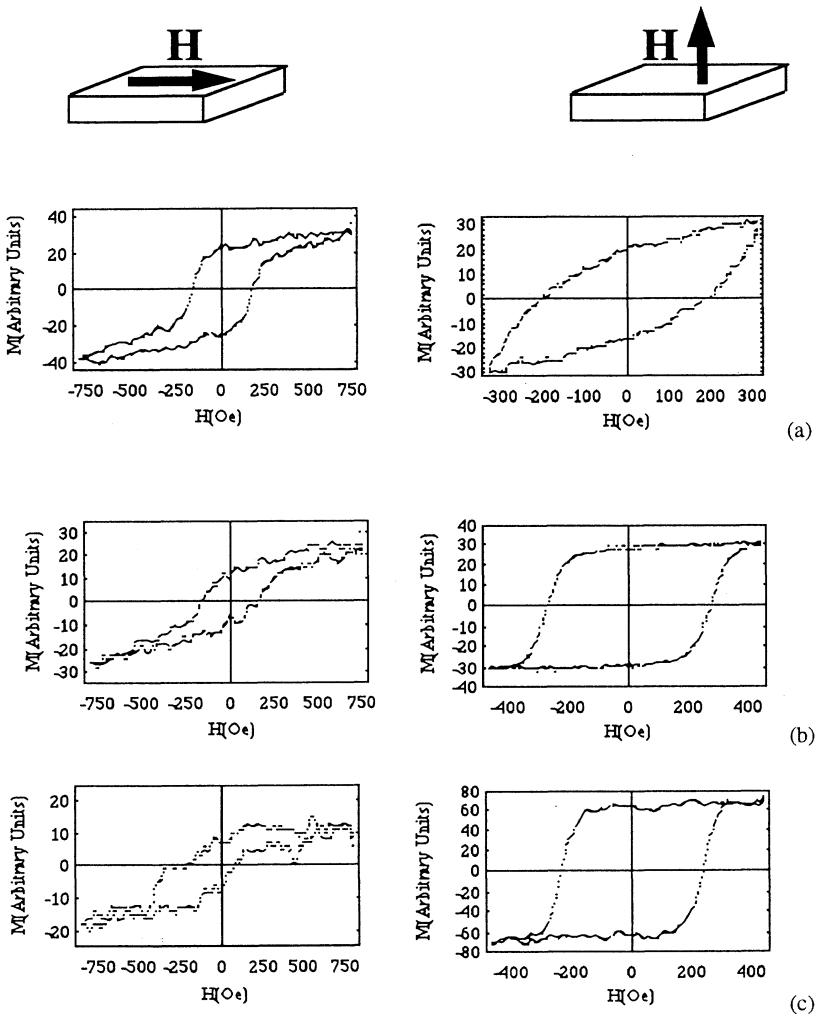

FIG. 9. (a) Longitudinal and polar MOKE loops of a 50 Å $Ni/Cu_{60}Ni_{40}$ (001) film. (b) Longitudinal and polar MOKE loops of a 35 Å $Ni/Cu_{60}Ni_{40}$ (001) film. (c) Longitudinal and polar MOKE loops of a 25 Å $Ni/Cu_{60}Ni_{40}$ (001) film.

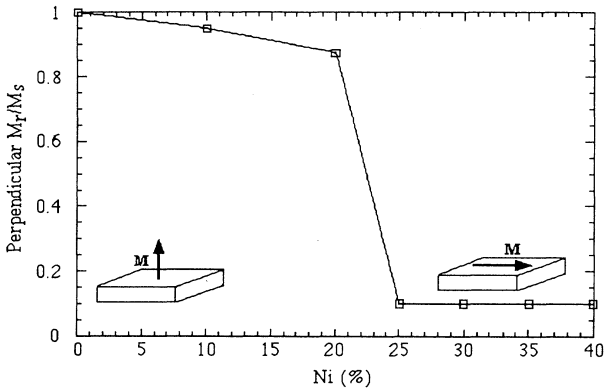

FIG. 10. Perpendicular remanence normalized to the saturation magnetization as a function of Ni atomic percent content in the substrate for the 100 Å $Ni/Cu_{1-x}Ni_x/Cu/Si$ (001) thin film characterized in air by VSM.

pendicular remanence gradually decreases and essentially vanishes for $x \geq 25\%$. One could think that as the Ni content in the substrate increases from 0 to 50 % and the misfit between the film and the substrate decreases from 2.6 to 1.3 % (Fig. 2), that the misfit strain in the 100 Å Ni film would decrease accordingly. However, Fig. 1 shows that according to the Matthews-Blakeslee model the misfit strain in the Ni film is the same in Ni/Cu (001) and in $Ni/Cu_{50}Ni_{50}$ (001), as long as the Ni thickness exceeds the critical thickness corresponding to $Ni/Cu_{50}Ni_{50}$ (001), which is 45 Å (Fig. 2). Also, even if the Matthews-Blakeslee model does not quantitatively predict the exact strain, it is clear that the misfit strain remaining in a 100 Å thick Ni film deposited on Cu(001) is small enough that its contribution to PMA is very weak. Therefore, the change observed in Fig. 10 is probably not due to differences in misfit strain. We believe that this significant change in magnetic anisotropy is rather due to the change of the chemical composition of the Ni-substrate interface. As one increases the Ni content x in the substrate, the $Ni\text{-}Cu_{1-x}Ni_x$ interface goes from being a Ni-Cu interface, for which we have determined $K^s \approx +0.85$ erg/cm^2, to an interface closer to Ni-Ni, which has zero surface magnetocrystalline anisotropy energy. Figure 10 implies that $K^s(Ni/Cu_{75}Ni_{25})$ (001) is small enough that $Ni/Cu_{75}Ni_{25}/Cu$ (001) cannot support perpendicular magnetization in a 100 Å thick Ni film exposed to air. This conclusion is consistent with the argument we used in the previous section for $Ni/Cu_{60}Ni_{40}$ thin films where the Ni thickness was variable but the alloy substrate composition was held fixed.

IV. CONCLUSIONS

We have studied the behavior of the magnetic anisotropy in $Ni/Cu_{1-x}Ni_x/Cu/Si$ (001) thin films ($0 < x < 50\%$) under UHV using MOKE and in air with VSM. We have discovered that the Ni/Cu (001) epitaxial system exhibits the largest thickness range of perpendicular magnetization of any epitaxial thin-film system reported so far. The extent of the perpendicular region is $10 < h_{Ni} < 60$ Å for vacuum/Ni/Cu/Si (001), 20 Å $< h_{Ni} <$ 40 Å for $Ni/Cu_{60}Ni_{40}/Cu/Si$ (001), $20 < h_{Ni} < 125$ Å for NiO/Ni/Cu/Si (001), and $20 < h_{Ni} < 135$ Å for Cu/Ni/Cu/Si (001). In fcc Fe/Cu (001) thin films, the perpendicular region extends only up to $h_{Fe} \approx 11$ Å. We have confirmed the very strong PMA in Ni/Cu (001) by MFM, which revealed the morphology and the size of the perpendicular magnetic domains in our thin films. The MFM images indicate a strong contrast between domains with the magnetization pointing into and out of the film plane. The magnetic domain structure is very complex and has two length scales: serpentine domains which are approximately 2 μm wide and submicron round bubble domains. To our knowledge, our measurements constitute the first observation of magnetic domains in ultrathin Ni/Cu (001) by MFM.

We have analyzed our results in terms of the strain-dependent Néel pair-interaction model of magnetic surface anisotropy. This analysis yielded the surface magnetocrystalline and the surface magnetoelastic anisotropy energies corresponding to the vacuum/Ni (001) ($K^s \approx -0.21$ erg/cm^2 and $B^s \approx +15$ erg/cm^2) and Ni/Cu (001) ($K^s \approx +0.85$ erg/cm^2 and $B^s \approx -50$ erg/cm^2) interfaces. We showed that the origin of the strong PMA in epitaxial vacuum/Ni/Cu (001), as in Cu/Ni/Cu (001) sandwiches, resides in the surface magnetocrystalline anisotropy of the Ni/Cu (001) interface and in the bulk magnetoelastic anisotropy energy of the Ni film, which is thickness dependent through the average in-plane biaxial misfit strain in the Ni. However, the PMA energy in the sandwiches is significantly larger than that in the vacuum/Ni/Cu (001) thin films leading to a broader perpendicular magnetic region. The large and negative surface magnetoelastic anisotropy energy of the Ni/Cu (001) interface is responsible for the in-plane magnetization at very small Ni thickness whereas the magnetostatic anisotropy causes the magnetization easy axis to fall in-plane at larger Ni thicknesses. The sign and magnitude of B^s(Ni/Cu) (001) implies that the effective magnetoelastic coupling coefficient changes sign at $h_{Ni} \approx 28$ Å in vacuum/Ni/Cu (001) thin films. Finally, we demonstrated that the onset of misfit dislocations is not responsible for the onset of perpendicular magnetization at small h.

ACKNOWLEDGMENTS

Gabriel Bochi gratefully acknowledges financial support by the NSERC of Canada. We thank Manfred Rührig and Steffan Porthun, University of Twente, for the preparation of the MFM tip. Technical assistance with the MFM measurements by I. Parashikov of the University of Basel is appreciated. This work was supported by NSF Grants No. DMR-9022572 and DMR-9410943, and ARO Grant No. DAAL 03-91-G0156.

[1]U. Gradmann, Ann. Phys. **7**, 91 (1966); J. Magn. Magn. Mater. **54**, 733 (1986); *Handbook of Magnetic Materials* (Elsevier Science, Amsterdam, 1993), Vol. 7, Chap. 1.
[2]J. G. Gay and R. Richter, Phys. Rev. Lett. **56**, 2728 (1986).
[3]A. J. Freeman and R. Wu, J. Magn. Magn. Mater. **100**, 497 (1991).
[4]N. C. Koon, B. T. Jonker, F. A. Volkening, J. J. Krebs, and G. A. Prinz, Phys. Rev. Lett. **59**, 2463 (1987).
[5]B. Heinrich, K. B. Urquhart, A. S. Arrott, J. F. Cochran, K. Myrtle, and S. T. Purcell, Phys. Rev. Lett. **59**, 1756 (1987).
[6]M. Stampanoni, A. Vaterlaus, M. Aeschlimann, and F. Meier, Phys. Rev. Lett. **59**, 2483 (1987).
[7]C. A. Ballentine, R. L. Fink, J. Arayat-Pochet, and J. L. Erskine, Appl. Phys. A **49**, 459 (1989).
[8]Z. Q. Qiu, J. Pearson, and S. D. Bader, Phys. Rev. Lett. **70**, 1006 (1993).
[9]D. Pescia, M. Stampanoni, G. L. Bona, A. Vaterlaus, R. F. Willis, and F. Meier, Phys. Rev. Lett. **58**, 2126 (1987).
[10]C. Liu, E. R. Moog, and S. D. Bader, Phys. Rev. Lett. **60**, 2422 (1988).
[11]D. P. Pappas, K.-P. Kämper, and H. Hopster, Phys. Rev. Lett. **64**, 3179 (1990).
[12]R. Allenspach and A. Bischoff, Phys. Rev. Lett. **69**, 3385 (1992).
[13]J. Thomassen, F. May, B. Feldmann, M. Wuttig, and H. Ibach, Phys. Rev. Lett. **69**, 3831 (1992).
[14]L. J. Swartzendruber, L. H. Bennett, M. T. Kief, and W. F. Egelhoff, Jr., in *Magnetic Ultrathin Films: Multilayers and Surfaces/Interfaces and Characterization,* edited by B. T. Jonker, S. A. Chambers, R. F. C. Farrow, C. Chappert, R. Clarke, W. J. M. de Jonge, T. Egami, P. Grünberg, K. M. Krishnan, E. E. Marinero, C. Rau, and S. Tsunashima, MRS Symposia Proceedings No. 313 (Materials Resreach Society, Pittsburgh, 1993), p. 237.
[15]B. N. Engle, C. D. England, R.A. Van Leeuwen, M. H. Wiedmann, and C. M. Falco, Phys. Rev. Lett. **67**, 1910 (1991).
[16]F. J. A. den Broeder, W. Hoving, and P. J. H. Bloemen, J. Magn. Magn. Mater. **93**, 562 (1991).
[17]C. H. Lee, Hui He, F. J. Lamelas, W. Vavra, C. Uher, and Roy Clarke, Phys. Rev. B **42**, 1066 (1990).
[18]R. Allenspach, M. Stampanoni, and A. Bischoff, Phys. Rev. Lett. **65**, 3344 (1990).
[19]T. Kingetsu and K. Sakai, Phys. Rev. B **48**, 4140 (1993).
[20]C. A. Ballentine, Ph.D. thesis, University of Texas at Austin, 1989.
[21]G. Bochi, C. A. Ballentine, H. E. Inglefield, S. S. Bogomolov, C. V. Thompson, and R. C. O'Handley, in *Magnetic Ultrathin Films: Multilayers and Surfaces/Interfaces and Characterization,* edited by B. T. Jonker, S. A. Chambers, R. F. C. Farow, C. Chappert, R. Clarke, W. J. M. de Jonge, T. Egami, P. Grünberg, K. M. Krishnan, E. E. Marinero, C. Rau, and S. Tsunashima, MRS Symposia Proceedings No. 313 (Materials Research Society, Pittsburgh, 1993), p. 309.
[22]F. Huang, M. T. Kief, G. J. Mankey, and R. F. Willis, Phys. Rev. B **49**, 3962 (1994).
[23]R. Naik, C. Kota, J. S. Payson, and G. L. Dunifer, Phys. Rev. B **48**, 1008 (1993).
[24]R. Jungbult, M. T. Johnson, J. aan de Stegge, A. Reinders, and F. J. A. den Broeder, J. Appl. Phys. **75**, 6424 (1994).
[25]G. Bochi, C. A. Ballentine, H. E. Inglefield, C. V. Thomspon, and R.C. O'Handley (unpublished).
[26]D. Pescia, G. Zampieri, M. Stampanoni, G. L. Bona, R. F. Willis, and F. Meier, Phys. Rev. Lett. **58**, 933 (1987).
[27]P. Krams, F. Lauks, R. L. Stamps, B. Hillebrands, and G. Güntherodt, Phys. Rev. Lett. **69**, 3674 (1992).
[28]B. M. Clemens, R. L. White, W. D. Nix, and J. A. Bain, in *Magnetic Thin Films, Multilayers, and Surfaces,* edited by S. S. P. Parkin, MRS Symposia Proceedings No. 231 (Materials Research Society, Pittsburgh, 1991), p. 459.
[29]D. S. Chuang, C. A. Balletine, and R. C. O'Handley, Phys. Rev. B **49**, 15 084 (1994).
[30]G. Bochi, O. Song, and R. C. O'Handley, Phys. Rev. B **50**, 2043 (1994).
[31]H. E. Inglefield, C. A. Ballentine, G. Bochi, S. S. Bogomolov, R. C. O'Handley, and C. V. Thompson, in *Thin Films: Stresses and Mechanical Properties IV,* edited by P. H. Townsend, T. P. Weihs, and J. Sanchez, Jr., MRS Symposia Proceedings No. 308 (Materials Research Society, Pittsburgh, 1993), p. 765.
[32]G. J. Mankey, M. T. Kief, and R. F. Willis, J. Vac. Sci. Technol. A **7**, 1595 (1991).
[33]Y. Chen, S. T. Tong, J. S. Kim, M. H. Mohamed, and L. L. Kesmodel, Phys. Rev. B **43**, 6788 (1991).
[34]H. E. Inglefield, G. Bochi, C. A. Ballentine, R. C. O'Handley, and C.V. Thompson (unpublished).
[35]J. W. Matthews and J. L. Crawford, Thin Solid Films **5**, 187 (1970).
[36]J. Y. Tsao, *Materials Fundamentals of Molecular Beam Epitaxy* (Academic, New York, 1993),Chap. 5.
[37]H. L. Davis, J. B. Hannon, K. B. Ray, and E. W. Plummer, Phys. Rev. Lett. **68**, 2632 (1992).
[38]C. Chappert and P. Bruno, J. Appl. Phys. **64**, 5736 (1988).
[39]P. Bruno and J.-P. Renard, Appl. Phys. A **49**, 499 (1989).
[40]L. H. Tjeng, Y. U. Idzerda, P. Rudolf, F. Sette, and C. T. Chen, J. Appl. Phys. **70**, 5939 (1991).
[41]C. K. Kim, Ph.D. thesis, Massachusetts Institute of Technology, 1991.
[42]H. E. Inglefield (unpublished).
[43]C. Kittel, Phys. Rev. **70**, 945 (1946).
[44]Y. Yafet and E. M. Gyorgy, Phys. Rev. B **38**, 9145 (1988).
[45]H. P. Oepen, M. Benning, H. Ibach, C. M. Schneider, and J. Kirschner, J. Magn. Magn. Mater. **86**, 137 (1990).
[46]H. J. Hug, Ph. D. thesis, Universität Basel, 1993.
[47]H. H. Hug, A. Moser, Th. Jung, A. Wadas, I. Parashikov, and H.-J. Güntherodt, Rev. Sci. Instrum. **64**, 2925 (1993).
[48]M. Rührig, S. Porthun, and J. C. Lodder, Rev. Sci. Instrum. **165**, 3225 (1994).
[49]S. Y. Chou, M. S. Wei, and P. B. Fischer, IEEE Trans. Magn. **30**, 4485 (1994).
[50]O. Song, C. A. Ballentine, and R. C. O'Handley, Appl. Phys. Lett. **64**, 2593 (1994).
[51]M. Weber, R. Koch, and K. H. Rieder, Phys. Rev. Lett. **73**, 1166 (1994).

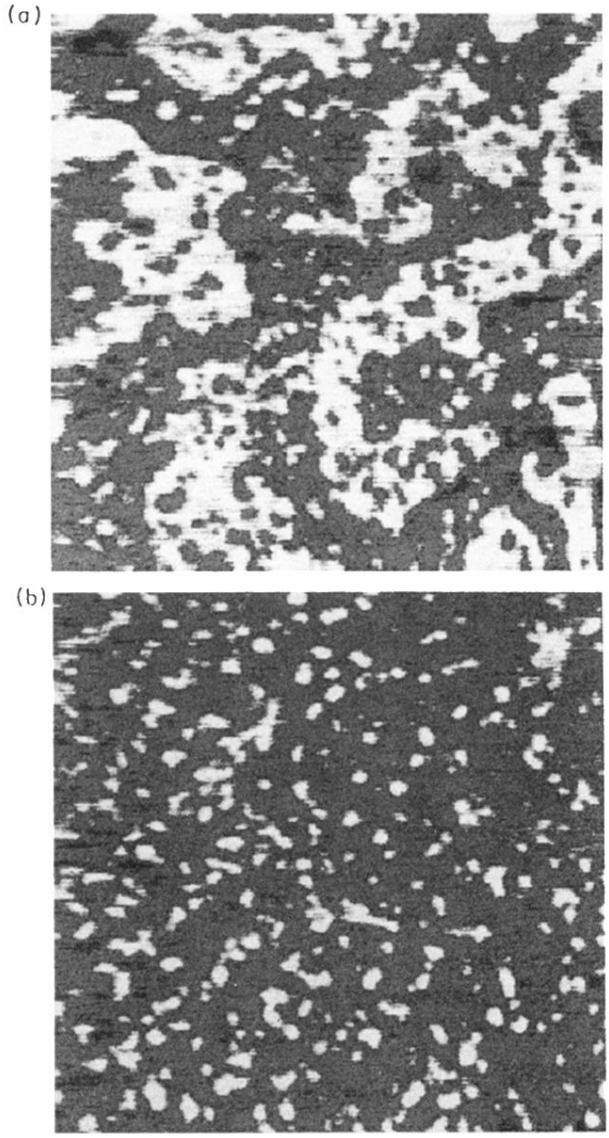

FIG. 5. (a) MFM image of the magnetic domain structure of a 20 Å Cu/100 Å Ni/2000 Å Cu/Si (001) sandwich. The light regions are perpendicular domains magnetized out of the plane of the film whereas the dark regions are perpendicular domains magnetized into the plane of the film. The up and down domains cover comparable surface areas indicating that the sandwich is demagnetized; (b) MFM images of the same sandwich after exposing it to a 4000 Oe magnetic field pointing into the plane of the film. The up domains shrink whereas the down domains grow. The field of view in both images is 10 μm $\times$10 μm.

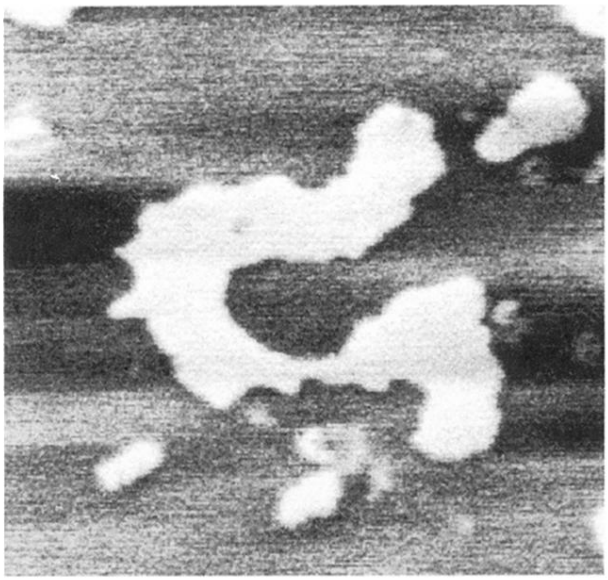

FIG. 6. MFM image of 20 Å Cu/85 Å Ni/2000 Å Cu/Si (001) sandwich. As in Fig. 5, the field of view of 10 μm $\times$ 10μm.